



Study on Geometric Nonlinearity of Spatial Beam Elements

Xiuhua Li¹, Siyang Li¹, Yongyi Yang^{2*}, Zhifu Liang³

¹ China Railway ERYUAN Engineering Group Co., Ltd, Chengdu, Sichuan 610031, China

²XIHUA University, Chengdu, Sichuan 610039, China

³Kunming Atide Software Co., Ltd, Kunming, Yunnan, 650106, China

*Corresponding author's e-mail: yongyiyang@136.com

Abstract. The analysis of geometric nonlinearity in structural engineering has gained increasing attention due to the growing complexity of modern structures, such as high-rise buildings, bridges, and aerospace components, which are often subjected to large displacements and rotations under extreme loading conditions. Spatial beam elements, in particular, play a critical role in these systems, yet their behavior remains challenging to model accurately because of the difficulty in distinguishing rigid body motion from actual deformation. This paper investigates the geometric nonlinearity of spatial beam elements, with a specific focus on structures experiencing significant displacements and rotations. To tackle this challenge, a co-rotational coordinate system is employed to isolate and compute the true deformation by subtracting rigid body translations and rotations, while a moving reference point method is introduced to efficiently handle coordinate transformations. Building on this theoretical foundation, a nonlinear structural analysis program (NSAP) was developed and rigorously validated through a test case involving a 45-degree spatial curved beam subjected to concentrated loading. The results demonstrate strong agreement with established commercial software such as ADINA and ANSYS, confirming the accuracy and reliability of the proposed approach. This work not only advances the understanding of geometric nonlinearity in spatial beam elements but also provides a novel and robust framework that can support future research and practical applications in nonlinear structural analysis.

Keywords: Nonlinear; Beam; Large Displacement

1 Introduction

The study of nonlinear behavior in three-dimensional (3D) beam structures has garnered significant attention in recent decades due to its critical relevance in modern engineering applications, such as high-rise buildings, long-span bridges, and flexible mechanical systems. Unlike linear analysis, which assumes small deformations and simplifies structural responses, nonlinear analysis accounts for large displacements, finite rotations, and material or geometric nonlinearities, providing a more accurate

representation of real-world structural behavior under extreme loading conditions. The complexity of spatial beam kinematics and the coupling of effects such as shear deformation, cable sag, and beam-column interactions necessitate advanced computational models and robust numerical methods to capture these phenomena effectively.

Recent advancements in nonlinear dynamics have provided valuable insights into the behavior of beam systems under complex conditions. For instance, Zhang et al. [1] explored the vibration reduction potential of an elastic beam coupled with an extension beam and a boundary nonlinear connector, highlighting the key role of nonlinear stiffness in controlling vibration responses. Their work demonstrated that a carefully designed nonlinear connector can effectively redistribute vibrational energy, offering a promising approach for engineering applications. Similarly, Chen et al. [2] investigated the forced vibration of a beam-plate system coupled through multiple nonlinear single-degree-of-freedom (SDOF) systems, revealing how nonlinear stiffness and damping influence low-frequency transverse vibrations. These studies underscore the importance of nonlinear coupling elements in altering the dynamic characteristics of beam-based structures.

In the context of rotating systems, He et al. [3] analyzed the dynamic behavior of a spinning Timoshenko beam-rigid disk system with nonlinear elastic boundaries under axial loading. Their findings emphasized the sensitivity of the system's response to nonlinear boundary parameters and initial conditions, illustrating the complexity of 3D beam dynamics in rotational environments. Furthermore, the identification of stiffness in beam structures with elastic foundations has been addressed by Yao et al. [4], who proposed a combined global mode and time-domain nonlinear subspace method to accurately determine both linear and nonlinear stiffness terms. This approach highlights the significance of precise parameter identification for reliable dynamic modeling of 3D beam systems. Additionally, Zhao et al. [5] introduced a nonlinear coupling oscillator to control the transverse vibration of a beam-plate system, demonstrating that adjustable nonlinear parameters can effectively suppress vibrations across coupled components. Additionally, the adoption of isogeometric analysis with NURBS basis functions has enabled the development of nonlinear spatial Bernoulli beam elements, capable of handling arbitrary cross-sectional orientations and large displacements with C^1 -continuity between elements [6]. These advancements underscore the growing sophistication of computational tools available for 3D nonlinear beam analysis.

This paper aims to contribute to the ongoing research by presenting a comprehensive study of spatial nonlinear analysis for 3D beam structures, integrating insights from finite element formulations, analytical solutions, and isogeometric approaches. Through a combination of theoretical derivations and numerical validations, we seek to address the challenges posed by large displacements and finite rotations, offering a framework that balances accuracy and computational efficiency for engineering applications.

The focus of this paper is the analysis of spatial beam elements undergoing large deformations. A primary challenge in this domain is accurately accounting for the effects of rigid body motion (translation and rotation) and distinguishing it from the actual deformation that generates internal forces. While existing methods, such as those relying on traditional fixed coordinate systems or simplified kinematic assumptions, have

advanced the field, they often exhibit limitations. These include insufficient precision in separating rigid body motion from deformation, particularly under large rotations, and computational inefficiency due to complex coordinate transformations or excessive reliance on iterative solvers. Such shortcomings can lead to errors in predicting internal forces and deformations, compromising the reliability of finite element analysis (FEA) for geometrically nonlinear structures. To overcome these limitations, this study adopts a co-rotational coordinate system that dynamically follows the rigid body motion of the element, enabling a more precise computation of true deformation by effectively isolating rigid body effects. Additionally, a moving reference point method is introduced to streamline transformations between coordinate systems, reducing computational overhead while maintaining consistency and accuracy.

2 Effects of Large Deformation

In finite element analysis of structural problems involving large displacements and rotations, the incremental nodal displacements induce motion in each element. This motion can be decomposed into three components: (1) rigid body translation of the element; (2) rigid body rotation of the element; and (3) the portion of motion that causes element deformation (i.e., the part that genuinely generates end forces in the element during computation). In geometric nonlinearity studies, most researchers adopt the Lagrangian coordinate system. In this system, the initial undeformed configuration of the object serves as the reference configuration, known as the Total Lagrangian (T.L.) formulation; alternatively, the last known equilibrium configuration at a given time step is used as the reference configuration, which changes with each computation, termed the Updated Lagrangian (U.L.) formulation [7, 8].

To accurately subtract the rigid body translation and rotation of the element, a coordinate system that follows the element's translation and rotation, called the co-rotational coordinate system, is attached to each element. At a given structural configuration at time t , the incremental nodal displacements from t to $t + \Delta t$ are calculated, and the rigid body translation and rotation are deducted from the nodal displacement increments for each element, yielding the portion of the nodal displacement increment that causes element deformation during t to $t + \Delta t$. Multiplying this portion of the nodal displacement increment by the tangent stiffness matrix of the element at time t provides the incremental end forces of the element during t to $t + \Delta t$.

The co-rotational (CR) formulation for planar beam elements has been thoroughly explained in many textbooks [9-12] and will not be repeated here. However, in 3D analysis, large rotations are not true vectors, and the rotation of element coordinate axes does not follow vector laws. The result of coordinate axis rotation depends on the sequence of rotations about each axis, making it impossible to directly extend the CR formulation for planar beam elements to spatial beam elements. In the following sections, three coordinate systems are established, and the nodal displacements in the element's co-rotational coordinate system are obtained using vector rotation transformations based on the relationships between these coordinate systems.

2.1 Three Coordinate Systems

To obtain the nodal displacements that genuinely cause element deformation after subtracting rigid body translation and rotation, three coordinate systems are established: (1) the structural coordinate system; (2) the element co-rotational coordinate system; and (3) the element end cross-sectional coordinate system.

The structural coordinate system serves as the foundational coordinate system for the entire structural computation. By solving the structural equilibrium equations, the translational displacements and rotational displacements ΔU_j , $\Delta \theta_j$, $j = 1, 2$, at nodes are obtained, where j denotes the endpoints 1 and 2 of the beam element.

The element co-rotational coordinate system is determined by the deformed position of the element, with its unit vectors denoted as e_i , $i = 1, 2, 3$. The element deformation, end forces, and stiffness matrix are defined in this coordinate system.

The element end cross-sectional coordinate system has unit vectors denoted as e_{ij}^s , $i = 1, 2, 3; j = 1, 2$. Each of the two endpoints of the element corresponds to a cross-sectional coordinate system. The origin of this coordinate system is at the centroid of the end cross-section, with the normal direction to the cross-section chosen as x_{1j}^s , and the principal axes of the cross-section as x_{2j}^s and x_{3j}^s .

The rotational deformation at the beam ends is determined by the rotation of these end cross-sectional coordinate systems relative to the element's co-rotational coordinate system. Clearly, at time $t=0$, when the structure has not undergone displacement, the element is in a stress-free state, and the end cross-sectional coordinate system coincides with the co-rotational coordinate system.

2.2 Calculation of End Cross-Sectional and Co-Rotational Coordinate Systems

For the sake of discussion, here is a brief introduction to the finite rotation formula. Let the initial position of vector R be represented by OP , with the unit vector along the direction of rotation denoted as n . After a rotation of angle ϕ around the n -axis, the resulting vector R' is represented by OQ . Thus, the finite rotation formula can be expressed as figure 1.

$$R' = ON + NV + VQ = n(n \cdot R) + [R - n(n \cdot R)]\cos\phi + (n \times R)\sin\phi \quad (1)$$

Using the finite rotation formula, the total rotation vector θ_j of the end cross-section at time $t + \Delta t$ is applied to the end cross-sectional coordinate system e_i at time $t=0$, yielding the unit vectors ${}^{t+\Delta t}e_{ij}^s$, $i = 1, 2, 3; j = 1, 2$ of the end cross-sectional

coordinate system at time $t + \Delta t$. The co-rotational coordinate system ${}^{t+\Delta t}x_1$ at time $t + \Delta t$ can be determined by the straight line passing through endpoints 1 and 2.

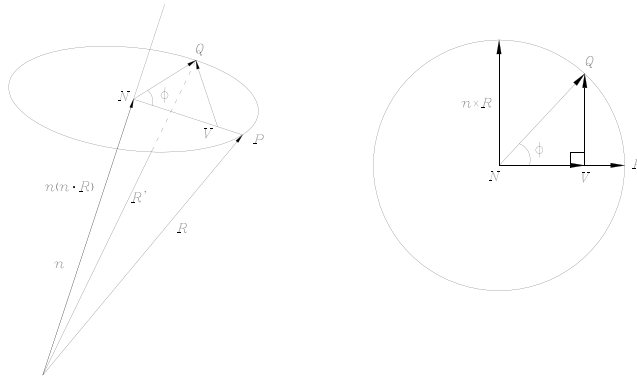


Fig. 1. Vector Diagram of Finite Rotation

An approximate method for calculating the basis vectors ${}^{t+\Delta t}e_2$ and ${}^{t+\Delta t}e_3$ of the co-rotational coordinate system is introduced first. Define the rotation vector θ_j^* from ${}^{t+\Delta t}e_1$ to ${}^{t+\Delta t}e_1^s$ as:

$$\theta_j^* = \arccos({}^{t+\Delta t}e_1 \cdot {}^{t+\Delta t}e_1^s) \frac{{}^{t+\Delta t}e_1 \times {}^{t+\Delta t}e_1^s}{|{}^{t+\Delta t}e_1 \times {}^{t+\Delta t}e_1^s|}, j = 1, 2 \quad (2)$$

Applying the rotation vector $-\theta_j^*$ to ${}^{t+\Delta t}e_{ij}^s, i = 1, 2, 3; j = 1, 2$, as shown in Figure 2. Clearly, ${}^{t+\Delta t}e_{1j}^s$ and ${}^{t+\Delta t}e_1$ coincides with the deformed chord direction, while ${}^{t+\Delta t}e_{2j}^s$ and ${}^{t+\Delta t}e_3$ represent the principal axis directions after pure torsion at the end cross-sections. Thus, the unit vectors ${}^{t+\Delta t}e_2$ and ${}^{t+\Delta t}e_3$ of the co-rotational coordinate system should be taken as the average of the two end cross-sections:

$${}^{t+\Delta t}e_i = \left({}^{t+\Delta t}e_{i1}^s + {}^{t+\Delta t}e_{i2}^s \right) / \left| {}^{t+\Delta t}e_{i1}^s + {}^{t+\Delta t}e_{i2}^s \right|, i = 2, 3 \quad (3)$$

Next, a precise method for calculating the basis vectors ${}^{t+\Delta t}e_2$ and ${}^{t+\Delta t}e_3$ of the co-rotational coordinate system is introduced. Define the rotation vector from ${}^{t+\Delta t}e_1$ to ${}^t e_1$ as θ_j^* , which can be computed using Equation (5). Applying the vector rotation

formula to ${}^t e_2$ and ${}^t e_3$ yields ${}^{t+\Delta t} e_2$ and ${}^{t+\Delta t} e_3$. At this point, all three basis vectors of the co-rotational coordinate system have been calculated.

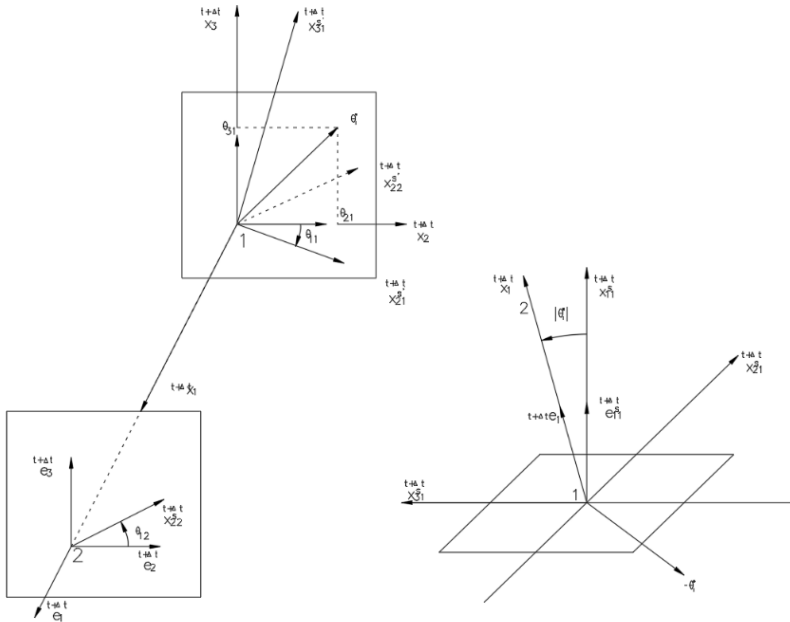


Fig. 2. Diagram of Co-Rotational System Calculation and Beam End Deformation

2.3 Calculation of Total Beam End Deformation

In the co-rotational coordinate system, element deformation can be decomposed into axial, bending, and torsional deformations.

(1) **Approximate Rotational Deformation Calculation:** Based on the assumption that the deformation rotations at the two endpoints of the beam element are small. Under this premise, the rotation vector θ_j^* obtained from Equation (5) is decomposed along the axes ${}^{t+\Delta t} x_i, i = 2, 3$ to obtain the bending deformation increment $\theta_{ij}, i = 2, 3; j = 1, 2$. Let $\theta_{1j}, j = 1, 2$ be the rotation vector from ${}^{t+\Delta t} e_2$ to ${}^{t+\Delta t} e_{2j}'$, which represents the torsional angle deformation increment at node j. From the above derivation, the following relationship is easily obtained $\theta_{11} = \theta_{12}$.

(2) **Precise Rotational Deformation Calculation:** Since rotational displacements are not vectors, they cannot be obtained by vector decomposition and synthesis between the global coordinate system and the co-rotational coordinate system. As shown in Figure 3, the rotational deformation $\theta_{ij}, i = 1, 2, 3; j = 1, 2$ at the two ends of the element

can be determined based on the relationship between the end cross-sectional coordinate system and the basis vectors of the co-rotational coordinate system.

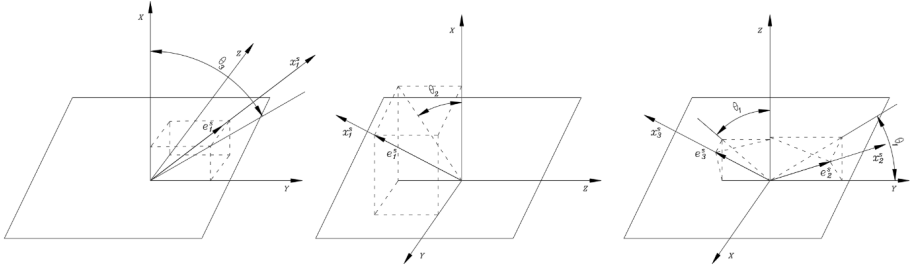


Fig. 3. Diagram of Rotational Deformation Calculation

The rotation deformation θ_{3j} about the z-axis is the angle between the projection of the vector x_1^s in the xoy-plane and the x-axis; the rotation deformation θ_{2j} about the y-axis is the angle between the x_1^s projection in the xoz-plane and the x-axis; and the rotation deformation θ_{1j} about the x-axis is the angle between the x_2^s projection in the yoz-plane and the y-axis. First, transform the basis vectors e_{ij}^s of the cross-sectional coordinate system to the local coordinate system:

$$\{v_{1j}, v_{2j}, v_{3j}\} = \left\{ {}^{t+\Delta t} e_{1j}^s, {}^{t+\Delta t} e_{2j}^s, {}^{t+\Delta t} e_{3j}^s \right\} r^s \begin{bmatrix} 1 & 0 & 0 \\ 0 & 1 & 0 \\ 0 & 0 & 1 \end{bmatrix} \quad (4)$$

where r^s is the transformation matrix from the cross-sectional coordinate system to the local coordinate system, expressed as:

$$r^s = \begin{bmatrix} \cos({}^{t+\Delta t} e_{1j}^s \cdot {}^{t+\Delta t} e_1) & \cos({}^{t+\Delta t} e_{1j}^s \cdot {}^{t+\Delta t} e_2) & \cos({}^{t+\Delta t} e_{1j}^s \cdot {}^{t+\Delta t} e_3) \\ \cos({}^{t+\Delta t} e_{2j}^s \cdot {}^{t+\Delta t} e_1) & \cos({}^{t+\Delta t} e_{2j}^s \cdot {}^{t+\Delta t} e_2) & \cos({}^{t+\Delta t} e_{2j}^s \cdot {}^{t+\Delta t} e_3) \\ \cos({}^{t+\Delta t} e_{3j}^s \cdot {}^{t+\Delta t} e_1) & \cos({}^{t+\Delta t} e_{3j}^s \cdot {}^{t+\Delta t} e_2) & \cos({}^{t+\Delta t} e_{3j}^s \cdot {}^{t+\Delta t} e_3) \end{bmatrix} \quad (5)$$

v_{ij} is the vector after transforming the basis vectors ${}^{t+\Delta t} e_{ij}^s$ of the cross-sectional coordinate system to the local coordinate system. The projection vectors of ${}^{t+\Delta t} e_{1j}^s$ in the xoy-plane, xoz-plane, and along the x-axis (v_{xy} , v_{xz} , v_x), and the projection vectors of ${}^{t+\Delta t} e_{2j}^s$ in the yoz-plane and along the y-axis (v_{yz} , v_y) are:

$$\{v_{xy} \quad v_{xz} \quad v_x\} = \begin{bmatrix} 1 & 1 & 0 \\ 1 & 0 & 1 \\ 1 & 0 & 0 \end{bmatrix} v_{1j} \quad (6)$$

$$\{v_{yz} \quad v_y\} = \begin{bmatrix} 0 & 1 & 1 \\ 0 & 1 & 0 \end{bmatrix} v_2 \quad (7)$$

The rotational deformations at the element end are then:

$$\theta_{3j} = a \cos \left(\frac{v_{xy} \cdot v_x}{|v_{xy}| \cdot |v_x|} \right) \quad (8)$$

$$\theta_{2j} = a \cos \left(\frac{v_{xz} \cdot v_x}{|v_{xz}| \cdot |v_x|} \right) \quad (9)$$

$$\theta_{1j} = a \cos \left(\frac{v_{yz} \cdot v_y}{|v_{yz}| \cdot |v_y|} \right) \quad (10)$$

(3) Axial Deformation: Assume that in the co-rotational coordinate system, the lateral deflection curve of the beam element follows a cubic (Hermitian) polynomial, the axial rotation varies linearly along the beam axis, and the membrane strain along the deformed beam axis is constant. Thus, the membrane strain can be calculated from the change in the arc length of the element.

The lateral deflection curves of the beam element are:

$$v(x_1) = N_1 u_{21} + N_2 \theta_{31} + N_3 u_{22} + N_4 \theta_{32} \quad (11)$$

$$w(x_1) = N_1 u_{31} - N_2 \theta_{21} + N_3 u_{32} - N_4 \theta_{22} \quad (12)$$

where v and w represent deflections in the x_2 and x_3 directions, respectively, and u_{ij} , θ_{ij} are the nodal displacements and rotations. $N_i, i = 1, 4$ are shape functions, expressed as:

$$\begin{aligned} N_1 &= \frac{1}{4(1-\xi)^2(2+\xi)} & N_2 &= \frac{c}{8(1-\xi^2)(1-\xi)} \\ N_3 &= \frac{1}{4(1+\xi)^2(2-\xi)} & N_4 &= \frac{c}{8(1+\xi^2)(1+\xi)} \end{aligned} \quad (13)$$

where c is the current chord length of the element, $\xi = -1 + 2x_i / c$ is the dimensionless coordinate, and x_{1j} is the nodal coordinates x_1 are in the co-rotational coordinate system $j, j = 1, 2$. The current arc length along the beam axis is:

$$S = \frac{c}{2} \int_{-1}^1 (1 + v^2 + w^2)^{1/2} dx_1 \quad (14)$$

2.4 Moving Reference Point Method

Through the above analysis, the deformation and incremental end forces in the co-rotational coordinate system have been obtained. However, the structural deformation is computed in the global coordinate system. Here, the moving reference point method is introduced to calculate the incremental end forces in the global coordinate system.

Using vector rotation, the three basis vectors ${}^{t+\Delta t} e_i, i = 1, 2, 3$ of the co-rotational coordinate system at time $t + \Delta t$ are obtained. Define the moving reference point coordinate as x_k, y_k, z_k . Clearly, the moving reference point must lie along the direction of the vector ${}^{t+\Delta t} e_2$ with an origin at some point on the element. Let the coordinates of a point on the element at time $t + \Delta t$ be ${}^{t+\Delta t} x_e, {}^{t+\Delta t} y_e, {}^{t+\Delta t} z_e$, and the vector length be 1, then:

$${}^{t+\Delta t} e_2 = (x_k - {}^{t+\Delta t} x_e)i + (y_k - {}^{t+\Delta t} y_e)j + (z_k - {}^{t+\Delta t} z_e)k \quad (15)$$

Using Equation (17), the reference point coordinates of the specified element at time $t + \Delta t$ can be determined, thereby obtaining the coordinate transformation matrix of the element.

3 Solution Methods for Nonlinear Equilibrium Equations

The basic methods for solving nonlinear equilibrium equations include the incremental method, the iterative method, and the combined incremental-iterative method.

In nonlinear solutions, the most effective approach combines the advantages of the incremental and iterative methods, applying the load in stages and iteratively solving the structure at each load step, known as the incremental-iterative method. In co-rotational coordinate iteration, the external load is first divided into several incremental steps. At the start of each incremental load step, the elastic stiffness matrix, geometric stiffness matrix, and coordinate transformation matrix of the element are recalculated based on the structural displacements and end forces from the previous step. These are then assembled into the global stiffness matrix, which is decomposed, stored, and updated as needed for iterations within the current load step using an iterative method. During iteration, residual unbalanced forces from the previous step typically exist. To

maintain structural equilibrium, the new nodal step equilibrium forces are calculated at the start of each incremental load step based on the current load increment and the residual forces from the previous step.

Various convergence criteria exist in iterative computations, including displacement convergence, unbalanced force convergence, and energy convergence. This paper adopts the displacement convergence criterion, with the judgment standard as follows:

$$\text{Max}\left\{|\Delta q_1 / q_1|, \dots, |\Delta q_n / q_n|\right\} < 0.001, \text{ 且 } \text{Max}\left\{|\Delta q_1|, \dots, |\Delta q_n|\right\} < 0.000001m \quad (16)$$

The nonlinear computation in this paper uses the incremental-iterative method, with three iteration approaches: (1) tangent stiffness iteration; (2) constant stiffness iteration; and (3) hybrid tangent and constant stiffness iteration (i.e., performing tangent stiffness correction after n constant stiffness iterations).

4 Numerical Example

Based on the foregoing theory, the author developed a pure 64-bit nonlinear structural analysis program, NSAP (Nonlinear Structural Analysis Program), using VS2015 with MFC technology. This program is suitable for 3D nonlinear analysis of spatial structures. It supports multi-document editing, complies with Windows industrial standards, and features a user-friendly human-computer interface, embodying the visibility, interactivity, and responsiveness characteristic of Windows programs.

Using structural data from Reference [13], NSAP was employed for analysis. A concentrated load was applied along the z -axis at the free end, causing the beam to undergo large spatial bending and torsional deformation, as shown in Figure 4. The beam is a 45-degree curved beam in the X - Y plane with a radius of 100, a square cross-section of 1×1 , elastic modulus $E = 10^7$, and shear modulus $G = 5 \times 10^6$. The beam was divided into 10 elements, with a load increment of 10 per step. The computation results were satisfactory, and comparisons are presented in Table 1. The figures 4 and 5 show the beam configurations at initial time and after loading steps of 300, 600, 900, 1500, and 2400, with all data in the example being dimensionless.

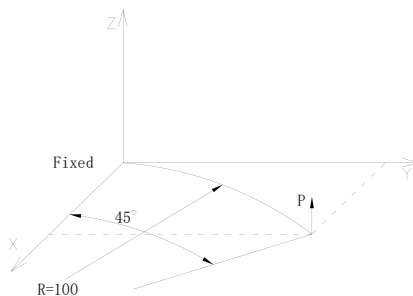


Fig. 4. Schematic of Loaded Curved Beam

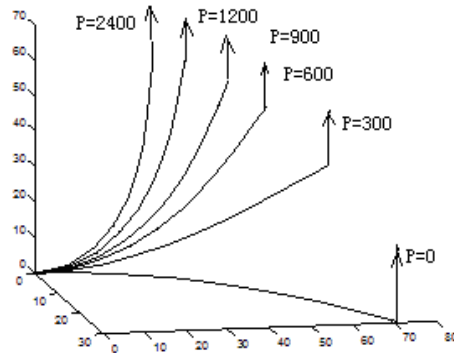


Fig. 5. Deformation Process of the 45-Degree Spatial Curved Beam

Table 1. Comparison of Free-End Coordinates of the 45-Degree Curved Beam After Deformation

P	ADINA-2			ANSYS			NSAP		
	x	y	z	x	y	z	x	y	z
0	29.3	70.7	0.0	29.3	70.7	0.0	29.3	70.7	0.0
300	22.2	58.5	40.4	22.15	58.57	40.45	22.23	58.44	40.47
600	15.7	46.8	53.6	15.60	46.92	53.62	15.89	46.65	53.57
900	---	---	---	11.83	39.83	59.12	12.25	39.50	59.01
1500	---	---	---	7.888	31.76	64.08	8.01	31.28	64.04
2400	---	---	---	5.206	25.52	67.36	5.366	25.07	67.28

5 Conclusion

This study successfully developed and implemented a method for analyzing the geometric nonlinearity of spatial beam elements. By employing a co-rotational coordinate system and the moving reference point method, we effectively addressed the challenges faced by traditional approaches in handling large displacements and rotations. Unlike existing methods that rely on fixed coordinate systems or simplified kinematic assumptions, our approach significantly enhances the precision of distinguishing rigid body motion from true deformation by dynamically tracking the element's rigid body motion, particularly excelling in scenarios involving large rotations. Furthermore, the introduction of the moving reference point method streamlines coordinate transformations, substantially reducing computational overhead compared to the complex transformations or excessive dependence on iterative solvers typical of conventional methods, while maintaining consistency and reliability in the analysis. The developed nonlinear structural analysis program (NSAP) demonstrated its effectiveness through a test case involving a 45-degree spatial curved beam under concentrated loading. The results from NSAP showed strong agreement with those from ADINA and ANSYS, further confirming the accuracy and practicality of this approach. This work contributes a comprehensive framework to the field of structural engineering, enabling more

efficient and precise handling of large deformation effects in spatial beam elements. The proposed methods and techniques are applicable to a wide range of structures, enhancing the capability of finite element analysis to address geometric nonlinearity. Future research could focus on extending this method to other element types, such as shells or solids, and exploring the coupled effects of material nonlinearity with geometric nonlinearity.

Acknowledgment

China Railway Science and Technology Research and Development Project (KSWQ224013)

Sichuan Provincial Natural Science Foundation, (No.:2023NSFC0389)

Yunnan Province Major Science and Technology Special Plan Project, (202302AD080009)

Yunnan Provincial Science and Technology Plan Project, (No.:202305AF150138)

Yunnan Provincial Science and Technology Plan Project, (No.: 202505AK340008)

References

1. Zhang, Z; Zhao, YH; (...); Li, Z. Vibration reduction study of an elastic beam by utilizing an extension beam and a boundary nonlinear connector[J]. *NONLINEAR DYNAMICS*, 2025.
2. Chen, MF; Guo, RS; (...); Zhao, YH. Forced vibration analysis of a beam-plate system coupled through multiple nonlinear single-freedom-degree systems[J]. *THIN-WALLED STRUCTURES*, 2024.
3. He, FF; Du, JT and Liu, Y. Dynamic behavior analysis of a spinning Timoshenko beam-rigid disk with nonlinear elastic boundaries under axial loading[J]. *NONLINEAR DYNAMICS*, 2024.
4. Yao, Y; Ma, ZS; (...); Liu, B. Stiffness identification of beam structures with elastic foundations through the global mode method and time-domain nonlinear subspace method[J]. *NONLINEAR DYNAMICS*, 2025.
5. Zhao, YH; Cui, HJ; (...); Sun, YH. A study of controlling the transverse vibration of a beam-plate system by utilizing a nonlinear coupling oscillator[J]. *THIN-WALLED STRUCTURES*, 2024.
6. Bauer, AM, Breitenberger, M, (...), Bletzinger, KU. Nonlinear isogeometric spatial Bernoulli beam [J]. *Computer Methods in Applied Mechanics and Engineering*, 2016, 303, pp. 101-127.
7. Huang Wen, Li Mingrui, Huang Wenbin. Geometric Nonlinear Analysis of Bar Structures—II: Three-Dimensional Problems. *Computational Structural Mechanics and Applications*, 1995, 12(2): 133-141.
8. Liu Lei et al. TL and UL Formulations in Nonlinear Analysis of Bar Structures. *Engineering Mechanics*, 2000 (Supplement): 361-365.
9. Pan Yongren. Geometric Nonlinear Static Analysis and Engineering Control of Suspension Bridges [Dissertation]. Tongji University, 1996.
10. Tang Maolin. Spatial Geometric Nonlinear Analysis and Software Development for Long-Span Suspension Bridges [Dissertation]. Southwest Jiaotong University, 2003.

11. Pan Yongren. Theory and Methods of Nonlinear Analysis of Suspension Bridge Structures. People's Communications Press, 2004.
12. Fan Lichu. Seismic Design of Bridges. Tongji University Press, 2001.
13. Bathe KJ, Bolourchi. Large Displacement Analysis of 3-D Beam Structures. International Journal for Numerical Methods in Engineering, 1979, 14(7): 961-986.

Open Access This chapter is licensed under the terms of the Creative Commons Attribution-NonCommercial 4.0 International License (<http://creativecommons.org/licenses/by-nc/4.0/>), which permits any noncommercial use, sharing, adaptation, distribution and reproduction in any medium or format, as long as you give appropriate credit to the original author(s) and the source, provide a link to the Creative Commons license and indicate if changes were made.

The images or other third party material in this chapter are included in the chapter's Creative Commons license, unless indicated otherwise in a credit line to the material. If material is not included in the chapter's Creative Commons license and your intended use is not permitted by statutory regulation or exceeds the permitted use, you will need to obtain permission directly from the copyright holder.

